

Preparation and study effect of vacuum annealing on structure and optical properties of AgCuInSe₂ thin film

R. H. Athab*, B. H. Hussein

Department of physics, College of Education for Pure Science / Ibn Al-Haitham, University of Baghdad, Baghdad, Iraq

Ag_{0.8}Cu_{0.2}InSe₂ (ACIS) alloys and thin films have been fabricated with different vacuum annealing temperatures Thin film has been deposited by thermal evaporation method of vacuum of 1.3*10⁻⁶ Torr with thickness about 700 nm at R.T and vacuum annealing at temperatures (373,473) K for 1 hour. The deposition in a vacuum on glass substrates. The crystal structure of deposited thin film had been examined by XRD and AFM analysis, which confirms the formation of tetragonal phase in 112 direction and these films are polycrystalline in nature having ideal stoichiometric. The optical properties of these films are determined for the wavelength range 400 - 1000 nm. The band gap of the Ag_{0.8}Cu_{0.2}InSe₂ films was evaluated to be (1.48-1.42) eV.

(Received June 11, 2022; Accepted October 12, 2022)

Keywords: Optical properties, AgCuInSe₂, AFM, Thin film

1. Introduction

Thin films photovoltaic technology is based on various types of light absorbers semiconductors. The I-III-VI₂ semiconductor materials have global energy and environmental problems[1]. Ternary compounds AgCuInSe₂ and CuInSe₂ is direct band gap semiconductors crystallizing in the chalcopyrite structure, they are the nearest chemical and electronic properties are analogues to binary zinc blende II-VI [2,3], I-III-VI₂ semiconductors group involve two metals and one chalcogen[4]. It is founded to be candidate material for low cost solar cell absorber [1] These thin-film semiconductor has been attractive material for solar cells because of their low production costs, high absorption, and chemical flexibility that allows for the alteration of the bandgap [5] high optical absorption coefficient, high carrier mobility, long term optoelectronic stability [6] Their bandgaps are lies between 0.8 and 2.0 eV [7] and between 1.07 and 2.73 eV cover the entire solar spectrum which makes it an ideal system for multi junction solar cell [8] the crystal structure is tetragonal structure chalcopyrite with the lattice constant a =b= 6.102 Å and c = 11.69 Å of AgInSe₂ and a =b= 5.781 Å and c = 11.552 Å of CuInSe₂ [9,10]. Quaternary compound thin film of AgCuInSe₂ has been deposited by several methods such as molecular beam epitaxy [11] Hybrid magnetron sputtering /evaporation[8] pulsed laser [2] thermal evaporation [12,13] magnetron sputtering [14] direct current (dc) sputtered [6] The chalcogenide semiconductor family I-III-VI₂ is AgInSe₂, and CuInSe₂ have suitable band-gap energies, the attention of much recent research because of their excellent electrical and optical properties, very significant application in optical devices (linear and nonlinear), photovoltaic solar cell, NIR applications in addition to the preparation of solar cells device and Schottky diode [1,15] The ionic radii of Cu doping being smaller than the ionic radius of Ag ion is suitable dopant for AIS lattice because the lower ionic radii Cu⁺ (0.71Å) than Ag⁺ (1.29Å) So Cu is of great interest as a substitute for Ag, the structural, optical and electrical properties of AIS film could be controlled. [16,17]. This work concentrate for on fabrication of of Ag_{0.8}Cu_{0.2}InSe₂ by vacuum evaporation method and study the concentrate on the effect of annealing (473,573) K on their description using XRD, AFM, optical measurement.

* Corresponding authors: rana.hameed1104a@ihcoedu.uobaghdad.edu.iq
<https://doi.org/10.15251/DJNB.2022.174.1173>

2. Experimental

In this work, the Silver Ag, Copper Cu, Indium In and selenium Se elements stoichiometric proportions by weight (0.8:0.2:1:2) with high purity for quaternary compound ACIS then mix these four elements and put under pressure of (3×10^{-4} mbar) in tube of quartz, then electric oven (1300 K) for six hours used to complete the alloy (3 g) was higher than the melting temperature of AgInSe₂ & CuInSe₂ [18,19]. The Ag_{0.8}Cu_{0.2}InSe₂ thin films were prepared by using (E 306) thermal evaporation at RT deposited on glass substrates at R.T with 700 nm thickness then vacuum annealing temperatures (473 and 573) K for study the electrical, structural, and optical properties of ACIS thin films. X-ray diffraction XRD, AFM have characterized the structural morphology of the ACIS films. X-ray diffraction has been used to study the structure of these films by detailed 2θ from 20° to 80° with intervals of 0.05° , The interplanar spacing (d_{hkl}) of miller index (hkl) was estimated by using Bragg's law [20] and Scherer's Formula used to calculate the crystalline size C.S of the films [21, 22]:

$$2dhkl \sin\theta = n\lambda \quad (1)$$

$$C.S = \frac{0.9\lambda}{B\cos\theta} \quad (2)$$

B (FWHM). is the width of the diffraction peak at half maximum intensity.

Microstrain (ϵ) for fabricated thin films can be calculated from the equation below:

$$\epsilon = \frac{B\cos\theta}{4} \quad (3)$$

The dislocations density (δ) is defined as the length of dislocation lines per unit volume of the crystal and it can be determine from the formula below [23]:

$$\delta = \frac{1}{(C.S)^2} \quad (4)$$

Optical properties of thin film prepare, transmission and absorption spectrums in the range between (400 to 1000) nm has been noted, lambert law and Tauc equation have been used to determine the absorption coefficients α and the energy gap (E_{gopt}) respectively from absorption spectrum [24,25]:

$$\alpha h\nu = D (h\nu - E_g)^r \quad (5)$$

$$\alpha = 2.303 \frac{A}{t} \quad (6)$$

α : the absorption coefficient, $h\nu$ the incident photon energy, r : a parameter for the type of the optical transition. A : absorbance, t : thickness D is a constant depends on the temperature and the properties of the valence & conduction bands.

Optical Constants such as n refractive index, k : extinction coefficient, real part ϵ_r & imaginary part ϵ_i of dielectric constant can be considered by the relations below: [26,27,28]:

$$n = \left[\frac{4R}{(R-1)^2} - k^2 \right]^{1/2} - \frac{(R+1)}{(R-1)} \quad (7)$$

$$k = \frac{\alpha\lambda}{4\pi} \quad (8)$$

$$\epsilon_r = n^2 - k^2 \quad (8)$$

$$\epsilon_i = 2nk \quad (10)$$

3. Results and discussion

Figure (1) displays the XRD spectrum of the deposited $\text{Ag}_{0.8}\text{Cu}_{0.2}\text{InSe}_2$ thin films with a thickness (700nm) at R.T and (373,473) K. From this figure we can notice that the patterns show that all thin films before and after annealing have a polycrystalline with tetragonal structures and two peaks which correspond to reflection from (112) & (204) planes of ACIS strongest sharp peak corresponding to (211) at diffraction angle 25.95, all the peaks of diffraction can be assigned to ICDD 00-038-0952 card standard value. Another one noticeable peak (204) when diffraction angle 42.55 can observe. We can notice when annealing with temperatures (373&473) K the places for measured diffraction peak do not alteration significantly, but the intensities peaks increase with annealing and crystallite size become larger. This implies that crystalline films have been improved due to system regularity and reduced defects[21].

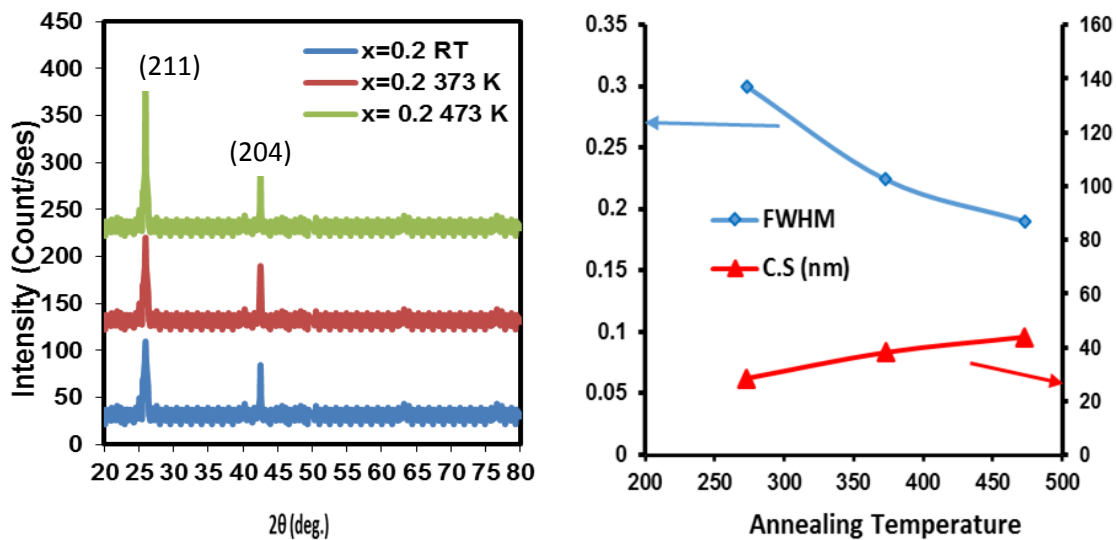


Fig. 1. XRD pattern for thin film $\text{Ag}_{0.8}\text{Cu}_{0.2}\text{InSe}_2$ at R.T and (373,473) K.

The crystallites size estimated by Scherer's formula is listed in Table (1) where it shows that the sample $\text{Ag}_{0.8}\text{Cu}_{0.2}\text{InSe}_2$ at 473 K have high crystallite size from other samples the decreases in FWHM of major peak which finally leads to increase in C.S of these films[29]. The decreasing in microstrain and dislocation density with increasing annealing temperatures (373&473) K. This is due to the direct proportionality between microstrain and FWHM of the main peak and the inverse proportionality between the dislocation density and the crystallite size. The decreasing in ACIS thin films defects with annealing temperature indicates improved their crystal structure.

Table 1. Experimental XRD data for thin films $\text{Ag}_{0.8}\text{Cu}_{0.2}\text{InSe}_2$ at R.T and (373,473) K.

T_a (K)	d_{exp} (Å)	$2\theta_{\text{exp}}$ (deg.)	hkl	FWHM (deg.)	C.S (nm)	$\delta \cdot 10^{15}$ (lines/m ²)	$\epsilon \cdot 10^{-3}$
R.T	3.42	25.95	112	0.2997	28.414	1.2385	73.012
	2.12	42.55	204				
373	3.42	25.95	112	0.22400	38.01	0.691908	54.570
	2.12	42.55	204				
473	3.42	25.95	112	0.195	43.67	0.524350	47.505
	2.12	42.55	204				

The surface morphology of the Ag_{0.8}Cu_{0.2}InSe₂ thin films at R.T and (373,473) K was examined by AFM analysis. Figure (2) shows analysis is a qualitative evaluation of the 3D shape and Granularity Cumulation Distribution chart images of these films.

Table 2. The grain size, roughness average and Root mean square of Ag_{0.8}Cu_{0.2}InSe₂ at R.T and (373,473) K.

Thickness (700nm)	Grain Size (nm)	Surfaces roughness (nm)	Root mean Sq. (nm)
R.T	79.07	16.3	19.2
373	85.66	16.6	19.7
473	86.52	18.7	22.1

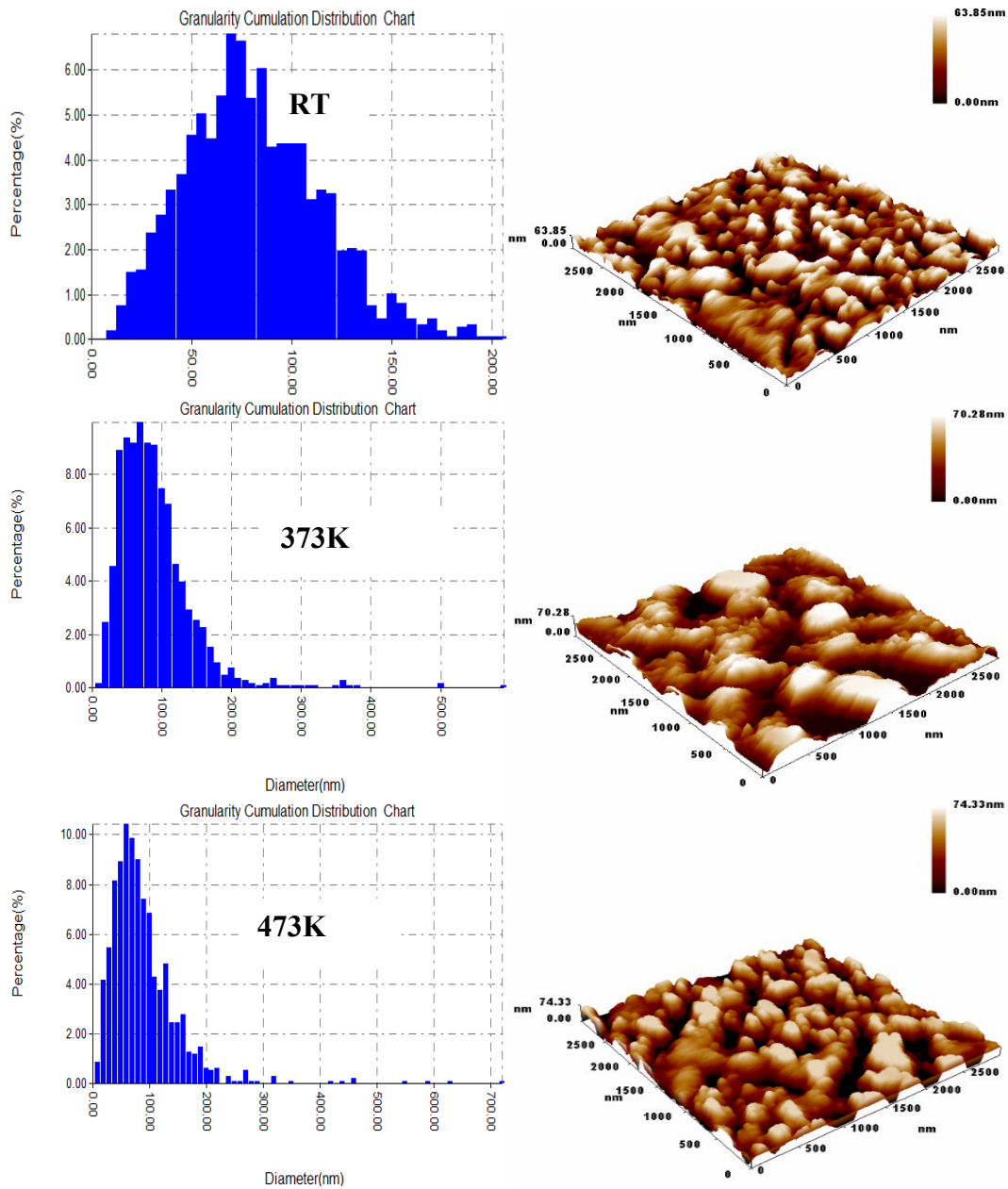


Fig. 2. Granularity Cumulation Distribution chart and three dimension Ag_{0.8}Cu_{0.2}InSe₂ at R.T and (373,473) K.

The obtained results clearly showed that these images with the crystalline grains were uniformly distributed throughout the surface Ag_{0.8}Cu_{0.2}InSe₂ thin films. The small particles have grown on the substrate surface and the pyramidal morphology variations can be seen. Thin films top surface roughness was important for evaluating thin films performance for device application. The observed physical dimensions of the structure such as average grain size (G.S), roughness and root mean square are listed in Table (2), the structures varied in average grain size from (79.07 to 86.52 nm) as well as to the variations in the roughness and root mean square values. It is clear from this table the average grain size, roughness and root mean square are increased after vacuum annealing thin film and the sample AICS have high value at 473 K. This behavior is due to the increase of the mobility of the atoms which causes the agglomeration of particles and of larger particles which in turn clues to a rise of the film roughness. These observations agree with XRD results.

The transmittance and absorbance spectra of the Ag_{0.8}Cu_{0.2}InSe₂ thin films at R.T and (373,473) K in the wavelength range of (400–1000) nm are displayed in Figure (3). we can notice the decrease in absorbance with increasing the λ for all samples. It can be seen that the transmittance values decrease when increases of vacuum annealing temperatures which means after annealing the absorbance values for these thin films are increasing, the photons absorption by free carrier contributed to the decrease in optical transmittance, or might be attributable to the growth of the crystallite size [30]. It is clear from figure 3 that the absorbance value of prepared Ag_{0.8}Cu_{0.2}InSe₂ thin film after annealing are near to 90%, these high values make these films a desired material for photovoltaic applications. Ag_{0.8}Cu_{0.2}InSe₂ film at 473 K has the highest values when the range of wavelength (400-600) nm, this behavior can be related to XRD and AFM data to understand the correlation between surface morphology and the increasing in absorbance [25].

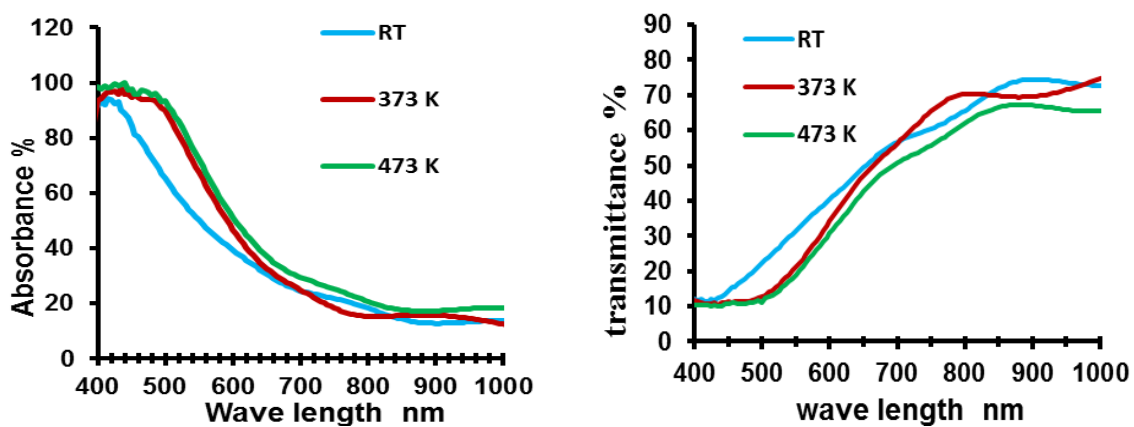


Fig. 3. The Absorbance and Transmittance spectrum of Ag_{0.8}Cu_{0.2}InSe₂ at R.T and (373,473) K.

The Tauc equation was used to compute the energy gap. This can be done by extrapolation to zero absorption in the Tauc equation. The variation of Eg Ag_{0.8}Cu_{0.2}InSe₂ thin films at R.T and (373,473) K is illustrated in figure (4). The allowed direct transition optical energy gaps of Ag_{0.8}Cu_{0.2}InSe₂ films were calculating from 1.48 eV to 1.42 eV good agreement with [4,6,31]. This means decreased the energy band gaps for vacuum annealed samples. It is decreased this decreed due to the dopant atoms at the grain boundaries and more absorbance can be get in Ag_{0.8}Cu_{0.2}InSe₂. The absorption coefficient α calculated from exponential law the Urbach law. In this present study the α values before and after vacuum annealing show in Table (3), the high value is $3 \times 10^4 \text{ cm}^{-1}$ for Ag_{0.8}Cu_{0.2}InSe₂ film at 473 K These values indicate the increasing of localized states in the band gap after the annealing.

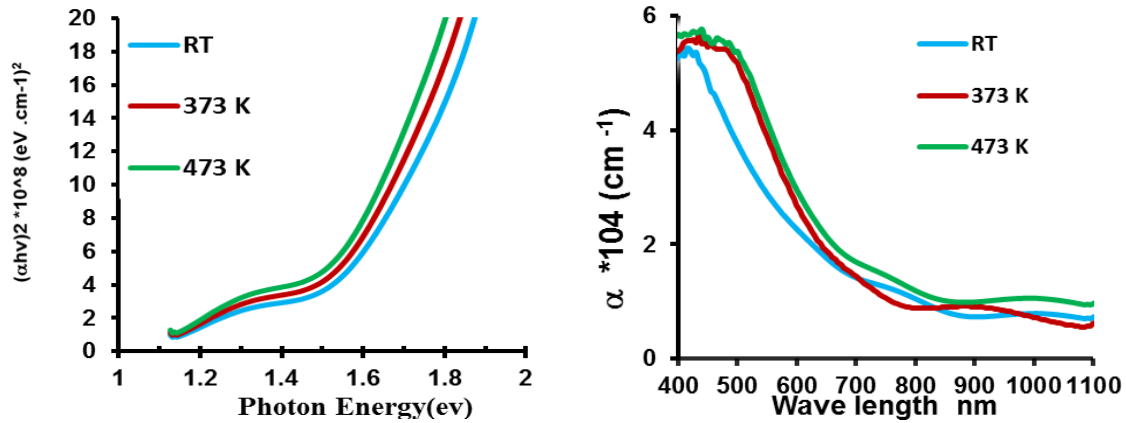


Fig. 4. The $(\alpha h\nu)^2$ with photon energy E_g and absorption coefficient with photon energy of $Ag_{0.8}Cu_{0.2}InSe_2$ at R.T and (373,473) K.

Table 3. The optical parameters (E_g^{opt} , α , k , n , ϵ_r and ϵ_i) for $Ag_{0.8}Cu_{0.2}InSe_2$ at R.T and (373,473) K. where $\lambda=600nm$.

Thickness (700nm)	E_g^{opt} (eV)	$\alpha \times 10^4$ cm^{-1}	n	k	ϵ_r	ϵ_i
R.T	1.48	2.26	1.8	0.1	3.2	0.39
473	1.45	2.7	1.7	0.12	3.14	0.47
573	1.42	3.0	1.73	0.14	3.00	0.48

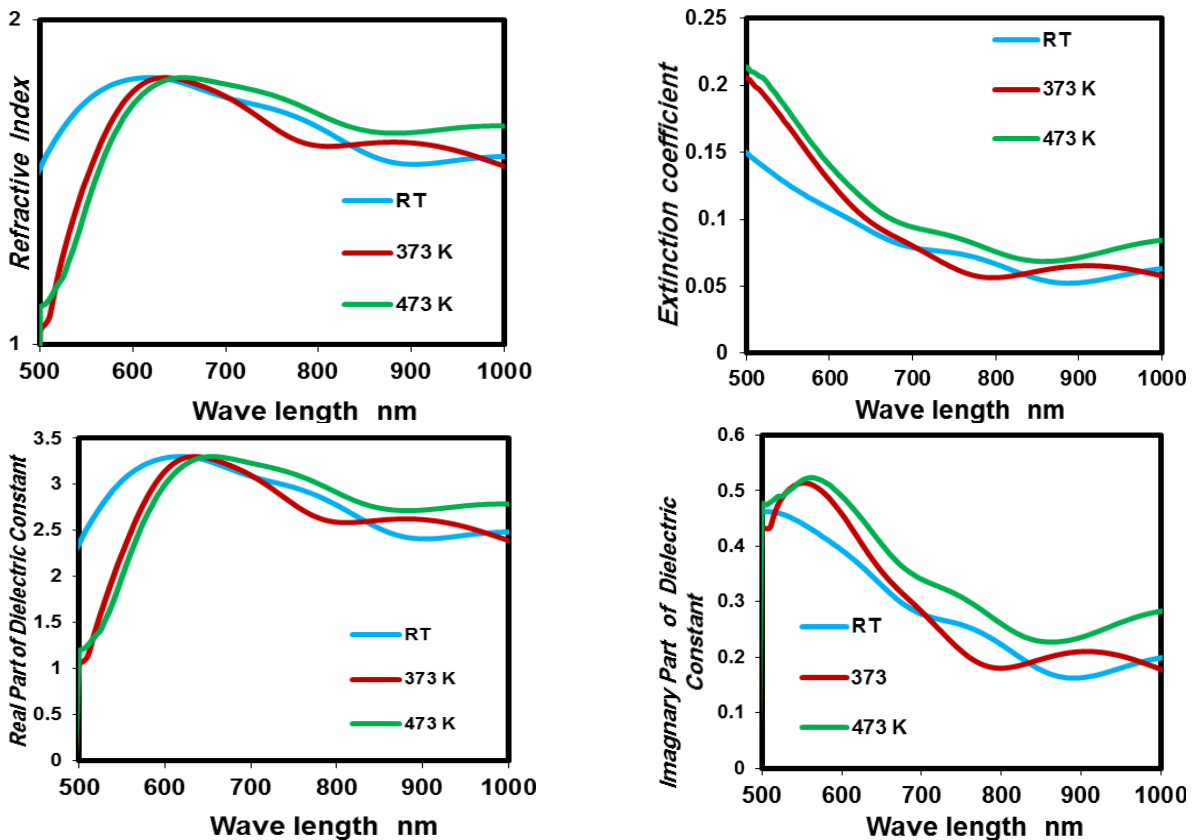


Fig. 5. Variation of refractive index, Extinction coefficient, of the real and imaginary part of dielectric constant with wavelength for $Ag_{0.8}Cu_{0.2} InSe_2$ at R.T and (373,473) K.

In order to determine optical constants are a significant parameter for optical material and application the value of the refractive index (n), the extinction coefficient (k) and the real and imaginary parts of the dielectric constant (ϵ_r , ϵ_i) for thin film $\text{Ag}_{0.8}\text{Cu}_{0.2}\text{InSe}_2$ at R.T and (373,473) K it calculated from equations of optical constants (7-10). The calculated values of optical constant at the wavelength (λ) equal to 600nm are listed in Table (3). The values of n decrease with vacuum annealing due to decrease the corresponding reflection this result agrees with [2,12]. The extinction coefficient increases as seen in Table (3) takes the same behavior of the absorption coefficient because the extinction coefficient is directly related to the absorption of the light. The fundamental electron excitation spectrum of the film was termed by means of the frequency dependency of the complex dielectric constant. The real (ϵ_r) dielectric constant related to the square of the refractive index observed for the smallest band gap value corresponds to the long-wavelength refractive index of the material [12]. The imaginary (ϵ_i) parts of the dielectric constant are related to the n and k values and the value of ϵ_r and ϵ_i at $\lambda=600\text{nm}$ decreases because the behavior of ϵ_r is similar to that of n , while the behavior of ϵ_i is similar to that of k because it mainly depends on the k value, the value of ϵ_i was smaller than of the thin film at RT, which indicates small dielectric loss. The best of optical constants was when vacuum annealing effect of 473 K.

4. Conclusions

Polycrystalline $\text{Ag}_{0.8}\text{Cu}_{0.2}\text{InSe}_2$ thin films were deposited on a glass substrate using thermal evaporation method at R.T and and the films were heat vacuum annealing at temperatures (373,473) K. The XRD study reveals the fact that $\text{Ag}_{0.8}\text{Cu}_{0.2}\text{InSe}_2$ thin films are crystalline in nature and tetragonal structure with preferential orientation (112) plane high crystallite size with 473 K. AFM studies reveal that the $\text{Ag}_{0.8}\text{Cu}_{0.2}\text{InSe}_2$ strongest effects on the morphology of the films as well as the crystallites grains are uniformly distributed throughout the surface for the deposited $\text{Ag}_{0.8}\text{Cu}_{0.2}\text{InSe}_2$ the average grain size increase after vacuum annealing. films display good absorption in the spectral range (400-700) nm. The band gap of the $\text{Ag}_{0.8}\text{Cu}_{0.2}\text{InSe}_2$ films was evaluated to be (1.48-1.42) eV this makes it is a promising way to enhance their properties to get suitable absorber layer for solar cell application.

References

- [1] P. Prabukanthan, M. Sreedhar, J. Meena, M. Ilakiyalakshmi, S. Venkatesan, G. Harichandran, A. Vilvanathaprabu, and P. Seenuvasakumaran, *J Mater Sci: Mater Electron* 32 6855-6865 (2021); <https://doi.org/10.1007/s10854-021-05390-y>
- [2] Valery Gremenok, Ivan Vasiljevich Bodnar, Ignacio Mártil, Felix L Martines, S.L. Sergeev-Nekrasov and I.A. Victorov, *Growth and characterization of $\text{Cu}_x\text{Ag}_{1-x}\text{InSe}_2$ thin films by pulsed laser Deposition*, *Solid State Phenomena*, 67-68, 361-366 (1999); <https://doi.org/10.4028/www.scientific.net/SSP.67-68.361>
- [3] Tinoco, T.; Rincón, C.; Quintero, M.; Pérez, G. S. N., *Physica Status Solidi A*. 124 (2): 427-434(1991); <https://doi.org/10.1002/pssa.2211240206>
- [4] F. A. Mahmoud and M. H. Sayed , *Chalcogenide Letters* 8 595 - 600 (2011).
- [5] Angel R. Aquino, Scott A. Little, Sylvain Marsillac, Rob Collins, and Angus Rockett, *IEEE*, 2011, 003532 - 003536.
- [6] Lin Rui Zhang, Tong Li, Hao Wang, Wei Pang, Yi Chuan Chen, Xue Mei Song¹, Yongzhe Zhang, and Hui Yan , *Superlattices and Microstructures*, 1-27 (2017)
- [7] Keiichirou Yamada, Nobuyuki Hoshino, Tokio Nakada, *Science and Technology of Advanced Materials*, 2006, 8, 595 - 600.
- [8] Angel R. Aquino, Angus Rockett, Scott A. Little, and Sylvain Marsillac, *IEEE*, 003586 - 003590 (2011)

- [9] Qian Cheng, Xihong Peng, and Candace K. Chan, *ChemSusChem*, 2013, 6, 102 – 109; <https://doi.org/10.1002/cssc.201200588>
- [10] S. Ferhi, M. F. Boujmil, B. Bessaïs, *EPJ Web of Conferences*, 2012, 29, 00017; <https://doi.org/10.1051/epjconf/20122900017>
- [11] Keiichirou Yamada, Nobuyuki Hoshino, Tokio Nakada, *Science and Technology of Advanced Materials* 7 42-45 (2006); <https://doi.org/10.1016/j.stam.2005.11.016>
- [12] H.H. Gullu, I. Candan E. Cos, kun M. Parlak, *Optik*, 1-30 (2015)
- [13] Hanan K. Hassun, *AIP Conference Proceedings*, 1968 (1) (2018)
- [14] T. Begou, S.A. Little, A. Aquino, V. Ranjan, A. Rockett, R.W. Collins, and S. Marsillac, *IEEE*, 000326 - 003528(2011)
- [15] Dingsheng Wang, Wen Zheng, Chenhui Hao, Qing Peng and Yadong Li, *The Royal Society of Chemistry*, 2556-2558 (2008).
- [16] R. D. Shannon, *Acta Crystallogr A.*, 32 (5), 751-767 (1976); <https://doi.org/10.1107/S0567739476001551>
- [17] N. N. Greenwood and A. Earnshaw, *Chemistry of the Elements*, Elsevier, (2012).
- [18] R. Panda, S. A. Khan, U. P. Singh, R. Naik and N. C. Mishra, *RSC Adv.*, 11, 26218-26227 (2021); <https://doi.org/10.1039/D1RA03409J>
- [19] O. Madelung, U. Rössler, M. Schulz, *Semiconductors · Ternary Compounds, Organic Semiconductors*, 41E, (2000); <https://doi.org/10.1007/b72741>
- [20] B. D. Cullity, *Elements of X-ray diffraction*, Addison-Wesley Pub. Co. Ind., London, 1967.
- [21] Wadaa S. Hussein, Ala' Fadhil Ahmed, Kadhim A. Aadim, *Iraqi Journal of Science*, 61 (6) 1307-1312 (2020); <https://doi.org/10.24996/ij.s.2020.61.6.8>
- [22] I. H. Khudayer and B.H. Hussien, *Ibn Al-Haitham J. for Pure & Appl. Sci.*, 29 (2), 41-51 (2016).
- [23] Chander, A. Purohit, C. Lal, and M.S. Dhaka, *Enhancement of Optical and Structural Properties of Vacuum Evaporated CdTe Thin Films*, *Mater. Chem. Phys.* 185, PP.202-209, (2017); <https://doi.org/10.1016/j.matchemphys.2016.10.024>
- [24] Bushra K. Hassoon Al-Maiyaly, *Ibn Al-Haitham J. for Pure & Appl. Sci.*, 29 (3), 14-25 (2016).
- [25] B. H. Hussein, H. K. Hassun, B. K.H. Al-Maiyaly, S. H. Aleabi, *Journal of Ovonic Research*, 18 (1), 37-41 (2022); <https://doi.org/10.15251/JOR.2022.181.37>
- [26] Bushra H. Hussein, Iman Hameed Khudayer, Mohammed Hamid Mustafa, Auday H. Shaban, *An International Journal (PIE)* 13(2), 173 (2019); <https://doi.org/10.1504/PIE.2019.099358>
- [27] S.Sze and K.Ng., *Physics of Semiconductor Devices*, 3rd edition, John Wiley and Sons, 2007; <https://doi.org/10.1002/0470068329>
- [28] B. K. H. Al-Maiyaly, B. H. Hussein, H. K. Hassun, *Journal of Ovonic Research*, 16 (5), 267 - 271 (2021).
- [29] H. I. Mohammed, I. H. Khdayer, I. S. Naji, *Chalcogenide Letters*, 17 (3) 107-115 (2020)
- [30] G. H. C. Radloff, F. M. Naba, D. B. Ocran-Sarsah, M. E. Bennett, K. M. Sterzinger, A. T. Armstrong, O. Layne, M. B. Dawadi, *Digest Journal of Nanomaterials and Biostructures*, 17 (2) 457 - 472 (2022).
- [31] Kihwan Kim, Seung Kyu Ahn, Jang Hoon Choi, Jinsoo Yoo, Young-Joo Eo, Jun-Sik Cho, Ara Cho, Jihye Gwak, Soomin Song, Dae-Hyung Cho, Yong-Duck Chung, Jae Ho Yun, *Nano Energy*, 2018.